



Characterization of Phosphate and Borate glasses with different additions, as optical band-Pass filters used for photometric detectors

Abeer Mahmoud EL- Maghraby¹, Eman Nabhan², Fatma Mohamad El-Sharkawy^{1*},
 Mohamed Shafic Khalil¹, Sawsaan. Mohamed EL- Mossalamy²,
Photometry Department; National Institute of Standards, Giza, Egypt¹
Physics Department; Faculty of sciences, Al-Azhar, University, Egypt²



CrossMark

Abstract

In this study three glass systems of chemical composition are used to obtain the band pass filter, Phosphate glass $40\text{P}_2\text{O}_5$ $40\text{ZnO}(19-x)\text{Na}_2\text{O}(x)\text{Cu}_2\text{O}$ 1CaO at ($x=0.5, 1, 2, 4, 6 \& 8\text{mol}\%$), Borate glass $40\text{B}_2\text{O}_3$ $40\text{ZnO}(19-x)\text{Na}_2\text{O}(x)\text{Fe}_2\text{O}_3$ 1CaO at ($x=0.5, 1, 1.5 \& 2\text{mol}\%$) and Lithium borate glass $75\text{Li}_2\text{B}_4\text{O}_7-x\text{Cu}_2\text{O}(25-x)\text{PbO}$ at ($x= 2.5, 5, 7.5 \& 10\text{mol}\%$). The amorphous nature of the samples was investigated using x-ray diffraction. Physical properties (density, molar volume, and Hardness) and infrared (IR) measurement of the composition of the glass was studied. The spectroscopic properties of the glass are investigated in UV-Visible range-near infrared range (from 300-800nm) using high accuracy spectrophotometer. We got a suitable glass composition that is close to the sensitivity of the human eye to visible light, which can be used as an optical filter such as a bandpass filter with a high sensitivity trap detector to measure photometric units.

Keywords:-Phosphate glasses, Borate glasses, Infrared, Hardness, photometric detectors.

1. Introduction

Phosphate glasses have very interesting physical properties compared to other glasses such as the low melting temperature, low glass transition temperature, high thermal expansion coefficients, high electrical conductivity, and optical characteristics [1-2]. Phosphate glasses also have the ability to accommodate high concentrations of modifiers or transition metal ions (TMI) and remain amorphous. [3-4]. They also have many important applications such as solid- state batteries, optical transmission, sensing laser technologies, optical amplifiers, nonlinear optics optical glass filter and sealing glass [5-6].

On the other side, phosphate glass has many disadvantages, the poor chemical durability is the main one, which limits its use in many applications [7-8]. The addition of transition metal oxide to phosphate glass has improved its chemical durability [9]. Previous studies [10-11], shows that, ZnO acts as a good glass modifier, because Zn ion acts as an anionic cross- linker between different phosphate anions, inhibiting hydration reaction [12]. The addition of transition metal ions to glasses has attracted much

attentions because of the ability of its ions to exist in more than one valence state, enabling electrical conduction to occur due to the movement of carriers from lower to higher valence state [13]. The electronic configuration in the ground state of copper, which is $(3d)^9$, is a good addition in an alkali-halide host crystal where Cu^+ is one such impurity that exhibits optical transmissions from 10 nm to 200nm. When the host cation with a larger ionic radius is substituted by Cu^+ ions, they occupy off-centered sites the ground state. The $3d-4s$ transition energy of Cu^+ is almost independent on the host crystal [14]. The observed color in the ternary glasses is the result of the absorption of copper ions in the glass due to $d-d$ electronic transitions.

Boron oxide is one of the most important glasses forming optical material because of its low cost, high transparency, high sensitivity, low melting point, high thermal stability, different coordination numbers, easy fabrication, shaping and mass production. The boroxol ring B_3O_6 is the dominant glass structure of the boron atoms in pure B_2O_3 . The addition of modifier to pure B_2O_3 breaks the boroxol ring and thereby produces

*Corresponding author e-mail: fsharkawy_2000@yahoo.com.

Receive Date: 02 June 2021, Revise Date: 20 June 2021, Accept Date: 21 June 2021

DOI: 10.21608/EJCHEM.2021.78880.3855

©2021 National Information and Documentation Center (NIDOC)

BO₃ and BO₄ units [15-17]. Borate glasses doped with TMI have many applications in microelectronics, optical glasses, and solid-state laser [18-20]. Recently many studies have indicated, that the glasses containing Fe₂O₃ are widely used in electrochemical, electronic, and electro-optic devices due to its unique electrical properties. However, the lack of information to explain the comprehensiveness on optical properties of Fe³⁺ doped glasses though many researchers have been carried out. The Fe₂O₃ also has strong absorptivity in the visible range [21]. A. Samir et al. had studied the effect of increasing CuO at the expense B₂O₃, Y. H. El Bashar and H. A. Abd El-Ghany had studied the effect of increasing Fe₂O₃ at the expense P₂O₅[22-23].

The aim of this work is to study the effect of the transition metal ions on the physical properties of the three studied glass systems which can use as a bandpass filters. That enable us to obtain a glass filter which resembles the V (λ) filter which is close to the sensitivity of the human eye in the visible light. These filters can be used with a trap detector for measuring photometric units in photometry lab in (National institute for standard). Also, these bandpass filters prevent ultra- violet and can use it as UV-laser protection [23].

2. Experimental procedures

2.1. Glass preparation

Sodium zinc phosphate glasses having the general formula $40P_2O_5 40ZnO (19-x) Na_2O(x) Cu_2O 1CaO$ with ($x=0.5, 1, 2, 4, 6 \& 8$) were prepared by the conventional melt–quench technique. Analytical grade ingredients of Na₂CO₃, ZnO, NH₄ H₂PO₄ and Cu₂O were used for glass preparation. Glass in formula $40B_2O_3 40ZnO (19-x) Na_2O(x) Fe_2O_3 1CaO$ with ($x=0.5, 1, 1.5 \& 2$) and Glass in formula $75Li_2B_4O_7-xCu_2O-(25-x) PbO_2$ with ($x=2.5, 5, 7.5 \& 10$) a series of samples of Li₂B₄O₇, PbO₂, Cu₂O were prepared with different compositions. It was started with composition 75mol% Li₂B₄O₇, 25mol% PbO₂ the concentration of copper oxide increased $x= 2.5, 5, 7.5, 10$ mol% at the expense of PbO₂. All three systems were prepared by the conventional melt–quench technique. The chemical reagents were thoroughly mixed and ground for (30–40) min in mortar pestle. Then the batch was melted in a porcelain crucible using a muffle furnace for (3–4) hours at a temperature ranging from 700 to

1100 °C depending on the composition. When the melt was thoroughly homogenized and attained desirable viscosity, it was poured onto the preheated brass plate. The prepared glass samples were annealed at appropriate temperatures (between 300 & 400 °C) for 2hour to remove the internal stresses. Then the samples were left inside the annealing furnace to cool slowly at room temperature.

2.2 X-ray diffraction analysis

XRD was carried out on glass powders to confirm the amorphous nature of the glasses. Measurements were carried out by X-ray diffraction model EMPYREAN equipped with Cu K α as radiation source ($\lambda=1.54 \text{ \AA}$). Data were collected using a detector at 2θ values from (5° to 90°), Power setting (40 mA, 40 kV).

2.3. Density and molar volume measurements

The densities of the prepared glass samples were determined at room temperature by the simple Archimedes method using toluene as immersing liquid ($\rho_o=0.863 \text{ g/cm}^3$). The glass densities ρ and molar volume V_m were calculated according to the following relation [24]:

$$\rho = [W_{air}/(W_{air}-W_t)] \rho_o; V_m = [M_w(\text{glass})/\rho_{\text{glass}}] \quad (1)$$

Where ρ_o is the density of the toluene and W_{air} & W_t are the sample weights in air and in the toluene, respectively. The measurement was repeated three times, and the average was taken

2.4 Hardness measurements

The hardness for glass samples was measured by (Shimadzu, HMV-2000). High polishing was essential to obtain smooth and flat parallel surfaces prior to indentation testing. Ten indentations were made and measured for each sample. The measurements were carried out under normal atmospheric conditions at $\approx 25^\circ\text{C}$. The appropriate loading 200 gm for a duration of 15 sec for all the studied glass samples. The micro hardness value was calculated using the formula [25].

$$H_v = A(P/D^2) \text{ kg/mm}^2 \quad (2)$$

Where,

A: is a constant takes into account the geometry of the square -based diamond indenter.

P: is the load in gm

D: is the average diagonal length in μm .

2.5 IR Measurements

The IR absorption spectra were registered at room temperature using a JASCO (FT/IR-6100) Fourier transform infrared spectrometer. The IR absorption measurements were carried out using the KBr pellet technique. In order to obtain good quality spectra, the samples were crushed in an agate mortar to obtain particles of micrometer size. The samples were mixed with KBr powder to make homogenous disks. The IR absorption spectra were measured immediately after preparing the disks. The IR spectra were recorded in the wavenumber range of 400-2400 cm^{-1} and normalized to eliminate the concentration effect of the power sample in KBr disk.

2.6 Optical measurements

Visible optical transmission spectra were measured for polished glass samples by a recording spectrophotometer in the range (300–800) nm, computer-controlled (SHIMADZU, UV-3101PC–UV–VIS–NIR Scanning Spectrophotometer).

3-Results and discussion

3.1 X-Ray Diffraction Analysis

XRD of the studied glass samples showed in Figure 1, was carried out to investigate the amorphous nature of the formulations produced. According to the XRD trace shown in Figure 1, there was a single broad hump centered on a low angle region of each composition, with no sharp peaks of the crystalline phase, detected in the XRD pattern, this confirmed that all the glasses produced were amorphous [26].

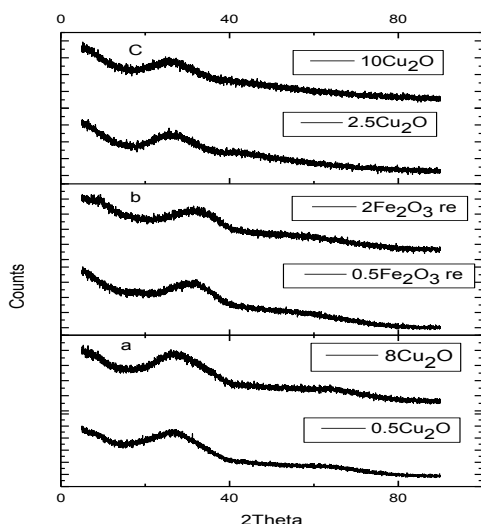


Figure 1: XRD pattern of the prepared: (a) $40\text{P}_2\text{O}_5-40\text{ZnO}-(19-x)\text{Na}_2\text{O}-1\text{CaO}-x\text{Cu}_2\text{O}$ (b) $40\text{B}_2\text{O}_3-40\text{ZnO}-1\text{CaO}-(19-x)\text{Na}_2\text{O}(x)\text{Fe}_2\text{O}_3$ (c) $75\text{Li}_2\text{B}_4\text{O}_7-x\text{Cu}_2\text{O}-(25-x)\text{PbO}_2$

3.2 Density and molar volume measurements

As the density is a basic property, but it is considered to be a very important and efficient tool capable of exploring the changes occurring in the structure of glasses. The density is affected by many factors such as the structural softening or compactness, the changes in geometrical configuration, coordination number of ions, and the dimensions of interstitial spaces of the glass [27]. The experimentally determined density is represented in figures 2(a, b & c) for the three studied groups. Both the experimentally density and the empirically calculated molar volume values are plotted in the same figure for comparison.

Figure (2-a) Shows that the density of the studied glass system increases as Cu_2O increases at the expense of Na_2O . This may be due to two reasons, the first the molecular weight of Cu_2O (143.091gm) greater than that of Na_2O (61.977gm), the second the cross-link increase due to that the Cu ion is divalent ion while Na is a monovalent ion, on the other hand, the molar volume decrease by substitution Na_2O by Cu_2O where ionic radii of Cu is less than of Na ($R_{\text{Cu}}=87\text{pm}$) ($R_{\text{Na}}=116\text{pm}$) [28]. The increase of cross-link density due to Cu_2O will cause compaction of the system which will reflect on the molar volume of the system to decrease.

In the same manner fig (2-b) shows that the density of the studied glass system increases as Fe_2O_3 increases at the expense of Na_2O . This may be due to two reasons: the first the molecular weight of Fe_2O_3 (159.692gm) is greater than that of Na_2O (61.977gm). The second, the cross-link increases due to Fe ions are divalent while Na ions are monovalent ion. On the other hand, the molar volume decreases by the substitution of Na_2O by Fe_2O_3 where ionic radii of Fe is less than of Na ($R_{\text{Fe}}=78.5\text{pm}$) ($R_{\text{Na}}=116\text{pm}$) [26]. The increase of cross-link density due to Fe_2O_3 will cause compaction of the system which will reflect on the molar volume of the system to decrease.

Figure (2-c) shows that the change in the density of such system is most likely related to the difference in the molecular weights of Cu_2O (143.091gm) and PbO (223.2gm)., the density decreases as the Cu_2O content increases. On the other hand, the molar volume VM shows the opposite trend. This may be due to the transformation of BO_3 to BO_4 as PbO is replaced by Cu_2O as will discussed in IR. The volume of BO_4 tetrahedral has much volume than

BO₃ which will increase the volume as Cu₂O increase content.

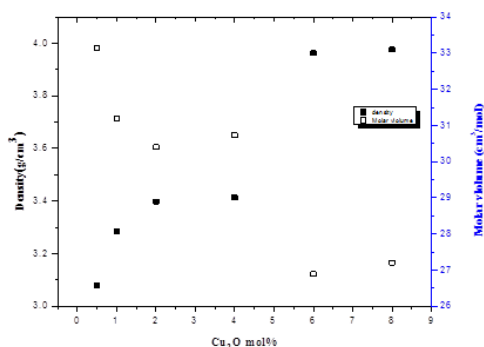


Figure (2-a): represent the relation between both Density and molar volume of (40P₂O₅-40ZnO-(19-x) Na₂O-1CaO-xCu₂O) glass samples.

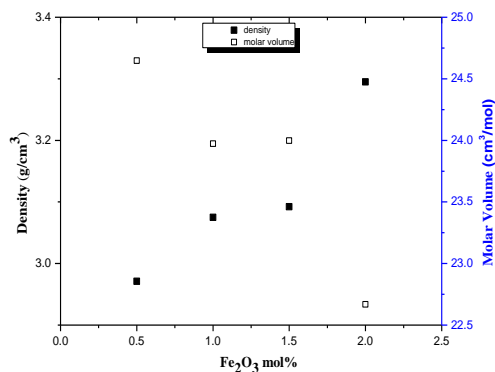


Figure (2-b): represent the relation between both Density and molar volume of (40B₂O₃ 40ZnO 1CaO (19-x) Na₂O(x) Fe₂O₃) glass samples.

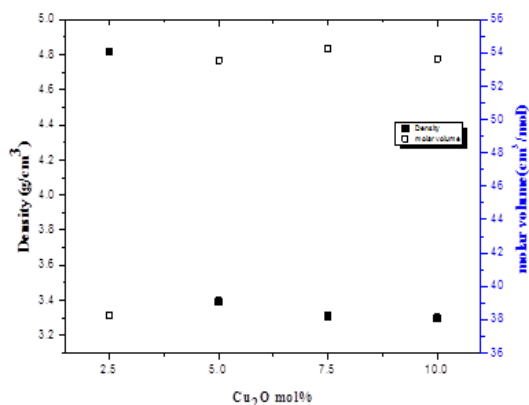


Figure (2-c): represent the relation between both Density and molar volume of (75 Li₂B₄O₇-xCu₂O-(25-x) PbO₂) glass samples.

3.3 Hardness measurements

Figure 3 (a, b, & c) represents the hardness of the three studied glass systems. These measurements are determined from Vickers Micro hardness.

Figure (3-a) shows that the hardness of the studied glass samples as a function of Cu₂O content. From the figure, the value of the hardness is found to be increased as Cu₂O content increases. It is known that the flow mobility of the constituent ions affects the hardness. The hardness increases as the flow mobility decreases. This was supported by the conclusion obtained from the hardness studies of E. Nabhan et al [29]. They suggested that the increase in the hardness number of different oxides are attributed to the decrease in the flow mechanism in a glass containing oxides. A decrease in the flow mobility is expected to occur in replacing Na₂O by Cu₂O due to the decrease in the non-bridging oxygen atoms resulting from the increase of the cross-link density as well as the remarkable difference of Na atomic mass, and the atomic mass of Cu and consequently the hardness increase.

Both Fe and Cu are divalent and have the same role. Figure (3-b) shows that, the hardness of the studied glass samples as a function of Fe₂O₃ content. Similarly, the value of the hardness is found to increase as Fe₂O₃ content increases. Similar to Cu₂O, the hardness increases due to the decrease in the flow mobility in replacing Na₂O by Fe₂O₃ due to the decrease in the non-bridging oxygen atoms resulting from the increasing of the cross-link density as well as the remarkable difference of Na atomic mass, and the atomic mass of Fe and consequently the hardness increase.

Figure (3-c) shows that the hardness of the studied glass samples as a function of Cu₂O content. From the figure, the value of the hardness is found to be increased as Cu₂O content increases. It is known that the flow mobility of the constituent ions will affect the hardness. The hardness increases as the flow mobility decreases. This may be also due to the transformation of BO₃ to BO₄ as PbO is replaced by Cu₂O as will discuss in IR.

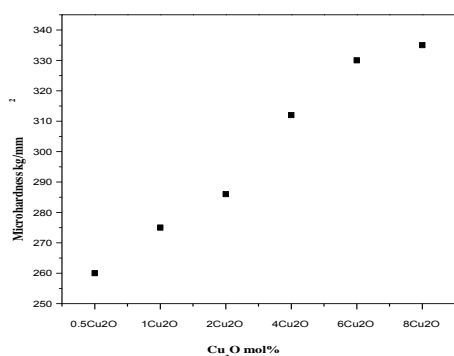


Figure (3-a): shows hardness of $40\text{P}_2\text{O}_5-40\text{ZnO}-(19-x)\text{Na}_2\text{O}-1\text{CaO}$ containing different amounts of Cu_2O . The hardness is increase by increasing concentration of copper.

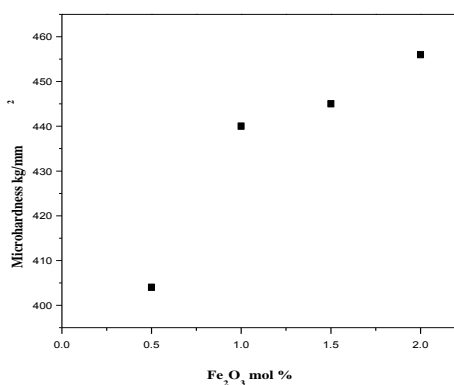


Figure (3-b): shows hardness of containing $40\text{B}_2\text{O}_3-40\text{ZnO}-(19-x)\text{Na}_2\text{O}-1\text{CaO}$ different amounts of Fe_2O_3 . The hardness is increase by increasing concentration of Fe_2O_3 .

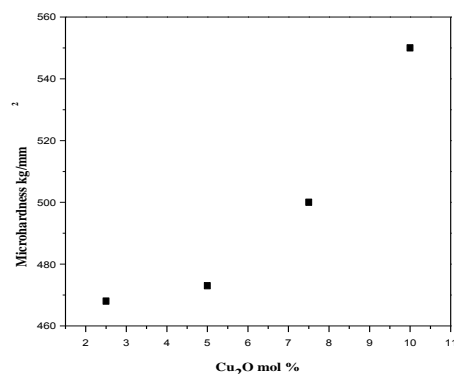


Figure (3-c): shows hardness of $75\text{Li}_2\text{B}_4\text{O}_7-x\text{Cu}_2\text{O}-(25-x)\text{PbO}_2$ containing different amounts of Cu_2O . The hardness is increase by increasing concentration of copper.

3.4 IR Measurements

The IR spectra of the studied glass samples in the range (400-2400) cm^{-1} have been measured and are shown in Figures (4, 5, & 6).

Figure(4) shows that IR absorbance spectra of $40\text{P}_2\text{O}_5-40\text{ZnO}-(19-x)\text{Na}_2\text{O}(x)\text{Cu}_2\text{O}-1\text{CaO}$ glass system where ($x=0.5, 1, 2, 4, 6$ and 8) there is a similarity between these spectra without any significant differences except a slight shift of bands position and sometimes changes in the relative intensities of the main bands are listed as follows.

-The band ranging from 460-600 cm^{-1} which can be assigned as bending vibrations of bridging phosphorus δ (O-P-O). This band intensity increases as Cu_2O increases this may be due to that the Cu^+ has absorption peaks at 590 and 520 cm^{-1} . This band is also found to be slightly shifted to lower wavenumber as Na_2O is replaced by Cu_2O [28-29].

-The broadband centered at 750 cm^{-1} which is assigned to a symmetric stretch of (P-O-P) bridges and slightly shifted to a higher wavenumber as Na_2O is replaced by Cu_2O [30-31].

-The band ranging from 880-900 cm^{-1} which assigned to asymmetric stretching of P-O-P is slightly shifted to higher wavenumber as Na_2O is replaced by Cu_2O . The higher shifted of both P-O-P symmetric and asymmetric may be due to the Cu ion increase the covalent character of the system as it increases [30-31].

-The band at 1000 cm^{-1} which is assigned to symmetric stretching of (P-O-) in PO_4 tetrahedra decrease until 4% mole Cu_2O and disappear as Cu_2O increase. This may be due to the decrease in non-bridging oxygen atoms due to the replacement of Na_2O by Cu_2O which increases the cross-link density in agreement with the density obtained from the density [30].

-The band at 1180 cm^{-1} which is assigned to symmetric stretch of (O-P-O) bridges in pyrophosphate groups is slightly shifted to higher wavenumber as the concentration of Cu_2O is increasing. This is may be due to the increase of the covalent character of the Cu ions ($\text{Cu-O} = 0.39$) [28, 38] and due to the decrease of the non-bridging oxygen atoms.

-The band at 1260 cm^{-1} which is assigned to an asymmetric stretch of (O-P-O) bond decrease in intensity and shifted to lower wavenumber by increasing the concentration of Cu_2O it was noticed that this peak is disappeared [31-33].

-The band at 1340 cm^{-1} which assigned to symmetrical vibration of (P-O) bonds, is shifted to lower wavenumber moreover, this band vanishes or merges with the band appeared at 1260 cm^{-1} [31-33].

Borate glasses have main three regions: The first region from 400-800 cm^{-1} which represents the bending group from 400-500 cm^{-1} and the linkage bending B-O-B at 700 cm^{-1} .

The second region from 800-1200 cm^{-1} which represents the stretching vibration of BO_4 groups. The third region from 1200-1500 cm^{-1} which is due to the stretching vibration of BO_3 groups.

Figure (5) shows that FTIR absorbance spectra of $40\text{B}_2\text{O}_3$ 40ZnO $(19-x)$ $\text{Na}_2\text{O}(x)$ Fe_2O_3 1CaO glass system where $(x=0.5, 1, 1.5 \text{ \& } 2)$ there is a similarity between the IR spectra without any significant differences except a slight shift of bands position and sometimes changes in the relative intensities of the main bands.

-The band from (400-500) cm^{-1} which can be assigned as bending vibrations of various borate arrangements, is shifted to lower wavenumber as Na_2O is replaced by Fe_2O_3 and its intensity changes as Fe_2O_3 increase [34-37].

-The band appeared at (700) cm^{-1} which can be assigned as linkages bending in borate network B-O-B is shifted to higher wavenumber as Na_2O is replaced by Fe_2O_3 , this may be due to the increase of the covalent character of Fe ion than Na ion [34-37].

-The band from (800-1200) cm^{-1} which can be assigned as (B-O) stretching vibrations of tetrahedral BO_4 units, is shifted to higher wavenumber as Na_2O is replaced by Fe_2O_3 [34-37].

-The band appeared from (1200-1500) cm^{-1} (Asymmetric stretching vibrations of B-O in trigonal BO_3 units) is shifted to higher wavenumber as Na_2O is replaced by Fe_2O_3 [34-37].

From fig (6) shows that IR absorbance spectra of $75\text{Li}_2\text{B}_4\text{O}_7$ $-x\text{Cu}_2\text{O}$ $-(25-x)$ PbO_2 glass system where $(x= 2.5, 5, 7.5 \text{ \& } 10)$ there is a similarity between the IR spectra without any significant differences except a slight shift the bands and sometimes changes in the relative intensities of the main bands.

-The band at 470 cm^{-1} which can be assigned as bending vibrations of B-O-B bond shifts to higher wavenumber as PbO_2 is replaced by Cu_2O [34-37].

- The band at 710 cm^{-1} which can be assigned as (B-O-B) Linkages bending in borate network shifts to higher wavenumber with increasing concentration of

Cu_2O the higher shift of both the band at 470 and 710 cm^{-1} may be due to the increase of the covalent character of Cu than Pb [34-37].

-The band appeared from 800-1200 cm^{-1} which can be assigned as (B-O-B) stretching vibrations of tetrahedral BO_4 units, its intensity increases as Cu_2O increase on the expense of PbO , this may allow to the transformation from BO_3 to BO_4 as Cu_2O increase this is an agreement with the density results .it is noticed that the broad shape of peak shifts to higher wavenumber with increasing concentration of Cu_2O .

-The band ranging from (1200-1500) cm^{-1} assigned to asymmetric stretching vibrations of trigonal BO_3 units shifts to higher wavenumber with increasing concentration of Cu_2O and its intensity decrease due to transformation from BO_3 to BO_4 as Cu_2O increase [34-37].

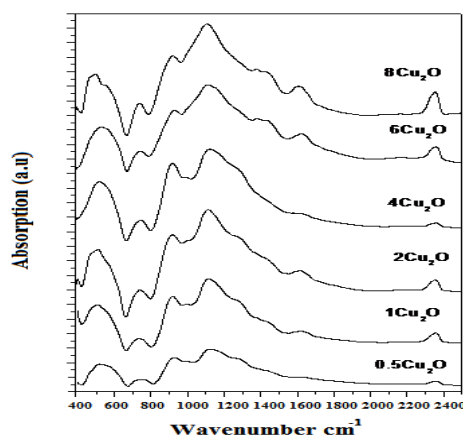


Figure 4: IR absorbance spectra of $40\text{P}_2\text{O}_5$ 40ZnO $(19-x)$ $\text{Na}_2\text{O}(x)$ Cu_2O 1CaO glass system where $(x=0.5, 1, 2, 4, 6 \text{ \& } 8)$

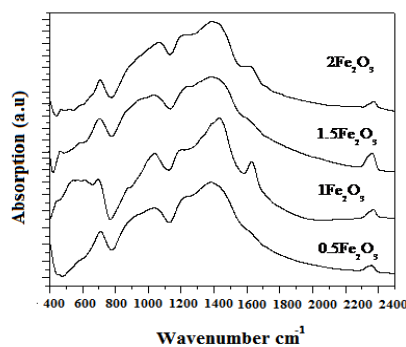


Figure 5: IR absorbance spectra of $40\text{B}_2\text{O}_3$ 40ZnO $(19-x)$ $\text{Na}_2\text{O}(x)$ Fe_2O_3 1CaO glass system where $(x=0.5, 1, 1.5 \text{ \& } 2)$

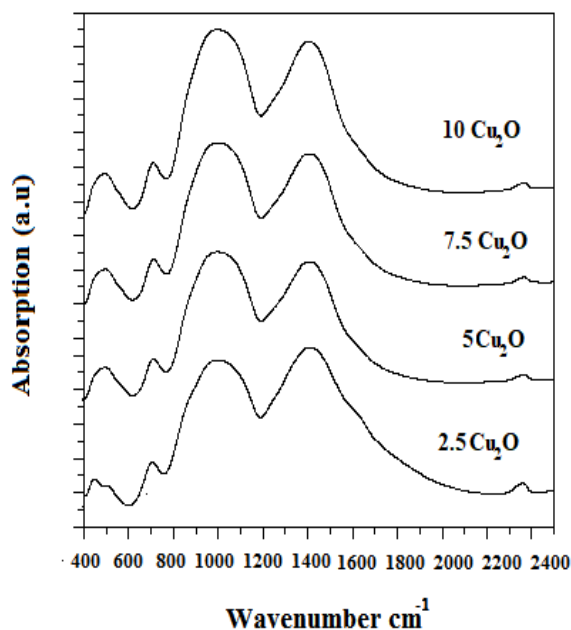


Figure 6: IR absorbance spectra of $75 \text{Li}_2\text{B}_4\text{O}_7 - x\text{Cu}_2\text{O} - (25-x) \text{PbO}_2$ glass system where ($x=2.5, 5, 7.5$ & 10)

3.5 Optical measurements

The transmission spectra of the studied glass samples are shown in figure (7). This figure illustrates that, the glass system $40\text{P}_2\text{O}_5 - 40\text{ZnO} - (19-x) \text{Na}_2\text{O} - 1\text{CaO}$ with different concentrations of Cu_2O shifted to lower transmission with higher wavelengths by increasing in concentration of copper. At concentration $0.5 \text{Cu}_2\text{O}$ and $1\text{Cu}_2\text{O}$ broad band pass filter appear. While at $2\text{Cu}_2\text{O}$ and $4\text{Cu}_2\text{O}$ there is a good band pass filter, the maximum at about 530nm but the tail of the curve does not cover all the visible range while at $6\text{Cu}_2\text{O}$ and $8\text{Cu}_2\text{O}$ there is a weak band pass with the small transmission. It was observed that the intensity decreases with the increase of copper concentration, this may be due to the decrease in transmission as Cu_2O concentration increases.

From figure (8) glass samples of optical transmission systematically shifted to lower transmission by increasing the concentration of Fe_2O_3 .

From the figure (9) the glass samples of optical absorption systematically shifted to lower transmission by increasing the concentration of copper. It was noticed from the figure that the curves are sharp and small bandwidth but not cover all the visible range but the concentration of $2.5\text{Cu}_2\text{OPb}$ cover all the visible range and the maximum at 570nm .

In order to obtain an optical pass filter, collect samples ($1\text{Cu}_2\text{O}$) in the phosphate system and sample ($1.5 \text{Fe}_2\text{O}_3$) in the borate system together then put inside the spectrophotometer holder to measure the transmission. Figure (10) illustrate the relation between the wavelength and the normalization (which we have got by divide the transmission value by the transmission value at 555nm) of the collected samples. It is observed that this figure is a band pass filter at a maximum 560nm and observed that the transmission curve cover all the visible range and this is the best result for our study.

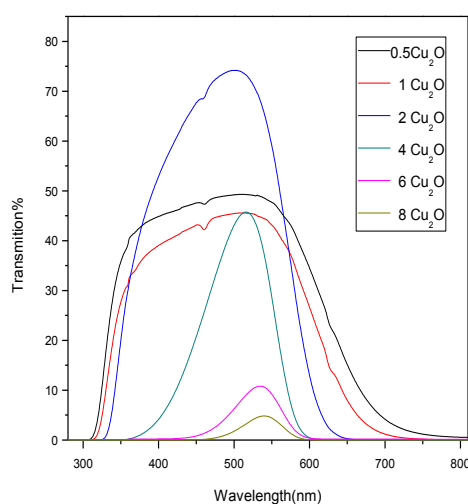


Figure7: shows the optical transmission spectra of $40\text{P}_2\text{O}_5 - 40\text{ZnO} - (19-x) \text{Na}_2\text{O} - 1\text{CaO}$ containing different amounts of Cu_2O .

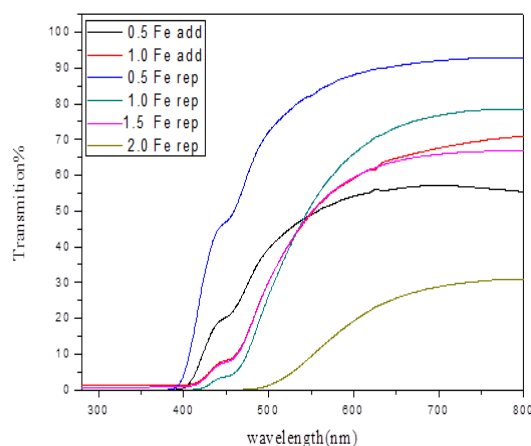


Figure 8: shows the optical transmission spectra of $40\text{B}_2\text{O}_3 - 40\text{ZnO} - (19-x) \text{Fe}_2\text{O}_3 - 1\text{CaO}$ containing different amounts of Fe_2O_3 .

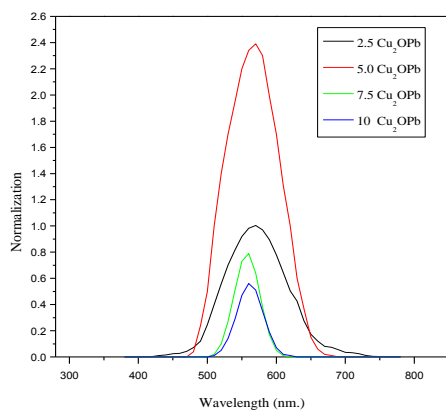


Figure 9: shows the optical transmission spectra of 75 $\text{Li}_2\text{B}_4\text{O}_7-x\text{Cu}_2\text{O}-(25-x)\text{PbO}_2$ containing different amounts of Cu_2O .

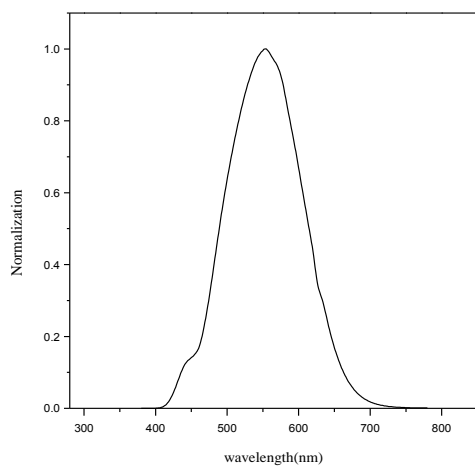


Figure 10: shows optical transmission spectra of collected sample ($1\text{Cu}_2\text{O} + 1.5\text{Fe}_2\text{O}_3$)

4-Conclusion

We prepared three composition of glass systems the first composition $40\text{P}_2\text{O}_5-40\text{ZnO}-(19-x)\text{Na}_2\text{O}-(x)\text{Cu}_2\text{O}1\text{CaO}[x=0.5, 1, 2, 4, 6, 8]$, the second composition $40\text{B}_2\text{O}_3 40\text{ZnO} (19-x)\text{Na}_2\text{O}(x)\text{Fe}_2\text{O}_3 1\text{CaO} [x=0.5,1,1.5,2]$ and the third composition $75\text{Li}_2\text{B}_4\text{O}_7-x\text{Cu}_2\text{O}-(25-x)\text{PbO}_2[x=2.5,5,7.5,10]$ all of them were prepared by the conventional melt-quench method.

- XRD pattern confirmed that all the glasses produced have an amorphous nature.

- The physical properties of all compositions were observed that both the first and the second

composition has an increase in the density value accompanied by an increase in the hardness value with an increase in the concentration of Cu_2O in the first and an increase in Fe_2O_3 in the second, in the third composition which has to decrease in the density value and despite that the hardness increased.

- The IR spectra show the presence of absorption bands of the studied glasses due to characteristic phosphate groups and borate groups. Through the optical study of the three compositions, we reached that ($1\text{Fe}_2\text{O}_3+1\text{Cu}_2\text{O}$) the best concentration achieves the desired goal of this study, which is to obtain an optical filter that is close to the sensitivity of the human eye to visible light. In this research, using limited possibilities, cheap materials, we obtained an optical filter. With increased laboratory potential, we can improve optical properties and this is what we aim for in the future.

References

- 1- Y. M. Mustafa and A. El. Adawy, "Structural and Physical Properties of Iron Oxichloride Phosphate Glasses" *Phys. Status Solidi A*, 179,83 (2000).
- 2- H. Elhaes, M. Attallah, Y. Elbasha, M. El-Okr, M. Ibrahim "Effect of glass structure on spin Hamiltonian parameters: Cu doped tellurite glasses" *Physica B* 449, 251-254 (2014).
- 3- E. Metwalli, M. Karabulut, D.L. Sideborton, M. M. Morsi and R.K. Brow "Properties and structure of copper ultraphosphate glasses" *J. Non-Crystalline Solids*, 344,128 (2004).
- 4- G. D. Khattak, E. E. Khavaja, L.E. Wenge, D. J. Thompson, M. A. Salim, A. B. Hallak and M. A. Daous," Composition-dependent loss of phosphorus in the formation of transition-metal phosphate glasses" *J. Non-Crystalline Solids* 1, 194 (1996).
- 5-A. G. Mostafa, M. Y. Hassaan, A. B. Ramadan, A. Z. Hussein and A. Y. Abdel-Haseib, "Characterization of Iron Sodium Phosphate Glasses Doped Ba^{2+} Cations for Using as Radioactive Waste Encapsulation" *J. Nature and Science*, 5, 148 (2013).
- 6-H. A. Saudi, A. G. Mostafa, N. Shata, S. U. El-Kameesy and H. A. Sallam," The structural properties of $\text{CdO-Bi}_2\text{O}_3$ borophosphate glass system containing Fe_2O_3 and its role in

- attenuating neutrons and gamma rays" *J. Physica B*, 406, 4001 (2011).
- 7- H. Yung, P.Y. Shih, H.S. Liu, T.S. Chin," Nitridation Effect on Properties of Stannous-Lead Phosphate Glasses" *J. Am. Ceram. Soc.* 80, 2213 (1997).
 - 8- M.R. Reidmeyer, M. Rajaram, D.E. Day," Preparation of phosphorus oxynitride glasses" *J. Non-Cryst. Solids* 85, 186 (1986).
 - 9- S.T. Reis, M. Karabulut, D.E. Day, "Chemical durability and structure of zinc-iron phosphate glasses" *J. Non-Cryst. Solids* 292, 150 (2001).
 - 10- D. Carta, J.C. Knowles, P. Guerry, M.E. Smith, R.J. Newport, "Sol-gel synthesis and structural characterisation of P₂O₅-B₂O₃-Na₂O glasses for biomedical applications" *J. Mater. Chem.* 19, 150 (2009).
 - 11- P. Pascuta, G. Borodi, N. Jumate, I. Vida-Simiti, D. Viorel, E. Culea," The structural role of manganese ions in some zinc phosphate glasses and glass ceramics" *J. Alloys Compd.* 504, 479 (2010).
 - 12- L. Montagne, G. Palavit, R. Delaval," Effect of ZnO on the properties of (100 - x) (NaPO₃)-xZnO glasses" *J. Non-Cryst. Solids* 223, 43 (1998).
 - 13- A.S. Shawaoush, A. A.Kutub, "An investigation of the electrical, optical and DSC properties of a copper-phosphate glass composition", *J. Mater. Sci.* 28, 5060 (1994).
 - 14- Joseph Simmons, Kelly S. Potter, *Optical Materials*, Academic Press, USA, Vol.1 (2000).
 - 15- I. Kashif, H. Farouk, A. S. Aly and A. M. Sanad, "Differential Scanning Calorimetry and Infrared Study of Barium Borate Glass Containing Transition Elements," *Physics and Chemistry of Glasses*, Vol. 32, No. 2, 77-78 (1991).
 - 16- A. C. Hannon, D. I. Grimley, R. A. Hulme, A. C. Wright and R. N. Sinclair, "Boroxol Groups in Vitreous Boron Oxide: New Evidence from Neutron Diffraction and Inelastic Neutron Scattering Studies," *Journal of Non-Crystalline Solids*, Vol. 177, No. 1, 299-316(1994).
 - 17- D. L. Griscom, "Borate Glass Structure," In: L. D. Pye, V. D. Fréchet and N. J. Kreidl, Eds., *Borate Glasses: Structure, Properties, Applications*, Plenum Press, New York, (1978) 11.
 - 18- C. Li and Q. Su, "Action of Co-Dopant in Electron-Trapping Materials: The Case of Sm³⁺ in Mn²⁺ Activated Zinc Borosilicate Glasses" *Applied Physics Letters*, Vol. 85, No. 12, 2190-2192 (2003).
 - 19- J.-M. Wu and H.-L. Huang "Microwave Properties of Zinc, Barium, and Lead Borosilicate Glasses," *Journal of Non-Crystalline Solids*, Vol. 260, No. 1-2, 116- 124 (1999).
 - 20- L. D. Bogomolova and M. P. Glassova, "The Impurity Effects in Vanadate Semiconducting Glasses," *Journal of Non-Crystalline Solids*, Vol. 37, No. 3, 423-426 (1980).
 - 21- Leong Pau Ming, Eeu Tien Yew, Leow Ting Qiao, Pang Xie Guan, Zuhairi Ibrahim & Rosli Hussin "Structural and Luminescence Properties of Fe³⁺ Doped Antimony Lead Borophosphate Glass" *Sains Malaysiana* 43(6) 915-922 (2014).
 - 22- A. Samir, Moukhtar A. Hassan, A. Abokhadra, L. I. Soliman, M. Elokr "Characterization of borate glasses doped with copper oxide for optical application" *Optical and Quantum Electronics* 51:123 (2019).
 - 23- Y. H. Elbashar, H. A. Abd El-Ghany "Optical spectroscopic analysis of Fe₂O₃ doped CuO containing phosphate glass" *Opt Quant Electron* (9) 49:310 (2017).
 - 24- S.F. Khor, Z.A. Talib, W.M. Mat Yunus "Optical properties of ternary zinc magnesium phosphate glasses" *Ceramics International* Volume 38, Issue 2, 935-940 (2012).
 - 25- A.M. Nassar, M.M. El Oker, Sh. N. Radwan and E. Nabhan "Effect of MO (CuO, ZnO, and CdO) on the compaction of sodium meta phosphate sealing glass". *Current Science International*, 2(2): 1-7, (2013).
 - 26- Hanan Elhaes, Mohamed Attallah, Yahia Elbashar, Ayser Al-Alousi, Mohamed El-Okr, and Medhat Ibrahim "Modeling and Optical Properties of P₂O₅-ZnO-CaO-Na₂O Glasses Doped with Copper Oxide" *Journal of Computational and Theoretical Nanoscience* Vol.11, No. 10, 2079-2084 (2014).
 - 27- Y. H. Elbashar • M. M. Rashad • D. A. Rayan "Physical and Mechanical Properties of Neodymium Doped Zinc Borate Glass with Different Boron Content Silicon" 10:115-122 (2018).
 - 28- Ionic radius data from R. D. Shannon, "Revised effective ionic radii and systematic studies of interatomic distances in halides and chalcogenides" *Acta Crystallographica* 32, no. 5, 751-767 (1976).

- 29-E. Nabhan, A. Nabhan, N. Abd El Aal. "Mechanical and Structural Properties of Zinc – Sodium - Phosphate Glasses Doped with Cu₂O" American Journal of Physics and Applications. Vol. 4, No. 6, 145-151 (2016).
- 30-A. Chahine, M. Et-Tabirou, M.Elbenaisi, M. Haddad, and J. L .Pascal "Effect of CuO on the structure and properties of (50-x/2) Na₂OxCuO (50-x/2) P₂O₅ glasses" Mater, Chem. Phys. 84, 341-347 (2004).
- 31-Xiuying Li, Anxian Lu, Huaming Yang" Structure of ZnO–Fe₂O₃–P₂O₅ glasses probed by Raman and IR spectroscopy" J. Non-Cryst. Solids 389, 21-27 (2014).
- 32- T. Jermoumi, S. Hassan, M. Hafid, "Structural investigation of vitreous barium zinc mixed metaphosphate" Vib. Spectrosc. 32 , 207–213 (2003).
- 33- P.Y. Shih, S.W. Yung, T.S. China, "FTIR and XPS studies of P₂O₅–Na₂O–CuO glasses"J. Non-Cryst. Solids 244, 211–222 (1999).
- 34- L. Balachander, G. Ramadevudu , Md. Shareefuddin , R. Sayanna, Y.C. Venudhar "IR analysis of borate glasses containing three alkali oxides" Science Asia 39 , 278–283 (2013).
- 35-Chand kiram Gautam, Avadhesh Kumar Yadav, and Arbind Kumar Singh "A Review on Infrared Spectroscopy of Borate Glasses with Effects of Different Additives"ISRN Ceramics Volume Article ID 428497, 17 pages,(2012).
- 36-Manal Abdel-Baki, Fouad El-Diasty "Role of oxygen on the optical properties of borate glass doped with ZnO" Journal of Solid-State Chemistry 184, 2762–2769 (2011).
- 37-Chenkai Zhu, Jinsong Liu, Songling Huang, Lizhe He, Xiaoye Cong, Chao Tan, Chris Rudd, Xiaoling Liu" The Effects of Fe₂O₃ and B₂O₃ on the Glass Structural, Thermal, in Vitro Degradation Properties of Phosphate Based Glasses" New Journal of Glass and Ceramics Vol 7, 100-115 (2017).